Impact of Radiation-Driven Optical Property Evolution on CubeSat Thermal Safety Margins in LEO

Sinyoung Park [a], Taeseok Kim [a,b,*]
[a]*Department of Electrical and Energy Engineering, Jeju National University, Jeju, 63243, Republic of Korea*
[b]*Department of Nuclear Engineering, Jeju National University, Jeju, 63243, Republic of Korea*
**Corresponding author: tkim@jejunu.ac.kr*

***Keywords : Radiation-induced degradation, SATMO, CubeSat thermal analysis, Low Earth Orbit (LEO)**

1. Introduction

With the advent of the New Space era, the commercial and academic utilization of CubeSats has rapidly expanded, and the importance of power and thermal management has correspondingly increased as mission complexity increases. Although CubeSats offer advantages in terms of low development cost and short implementation timelines, their miniaturized structure and constrained mass and power budgets make them highly sensitive to variations in the external thermal environment.[1]

Satellites operating in Low Earth Orbit (LEO) are exposed to a vacuum environment where convection is negligible, and heat transfer is predominantly governed by radiation. A CubeSat is exposed to multiple heat inputs, including direct solar flux, Earth albedo, Earth infrared (IR) radiation, and internal heat generation. As a result, the spacecraft experiences periodic heating and cooling over each orbital period.[2]

In particular, the β angle significantly influences the solar incidence condition and the overall thermal load, resulting in extreme thermal scenarios commonly referred to as the hot case and the cold case.

Under these space thermal conditions, the thermal behavior of a satellite is governed by the surface energy balance and can be expressed under steady-state conditions by the following radiative equilibrium equation:

$$\alpha(S + Q_{albedo}) + Q_{IR} + Q_{internal} = \varepsilon\sigma T^4 \qquad (1)$$

where σ is the Stefan–Boltzmann constant (5.67×10^{-8} W m^{-2} K^{-4}), and T is the surface temperature.[3]

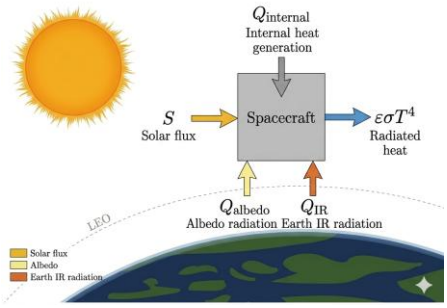

Fig. 1. Satellite surface energy balance schematic

Here, the solar absorptance (α) and infrared emittance (ε) are key optical properties that determine the equilibrium temperature of the spacecraft. Most CubeSats rely on passive thermal control materials, such as Optical Solar Reflectors (OSRs) and white thermal control coatings, to regulate heat. However, prolonged exposure to the space radiation environment, including ultraviolet (UV) photons and charged particles such as electrons and protons, can alter the optical properties of these materials.

Previous studies have reported an increase in solar absorptance and a decrease in infrared emittance for certain white coatings following irradiation.[4] Such changes simultaneously enhance heat absorption while reducing radiative heat rejection capability, potentially leading to an increase in spacecraft temperature.

Nevertheless, many small satellite thermal designs are still performed based on Beginning-of-Life (BOL) material properties, and quantitative thermal analyses incorporating End-of-Life (EOL) optical property degradation remain limited.

In the context of space nuclear power systems, accurate prediction of external thermal environments is essential for ensuring reliable system operation, as these environments define the boundary thermal conditions experienced by onboard components. Therefore, this study is positioned as a preliminary investigation for space nuclear power systems, focusing on quantifying how radiation-induced degradation of optical properties influences orbital temperature behavior and thermal safety margins. The proposed analysis framework can be further extended to system-level thermal analyses of space nuclear applications.

Accordingly, a systematic evaluation of the impact of radiation-induced optical property degradation on orbital temperature behavior and thermal safety margin is required.

2. Methodology

2.1 Thermal Analysis Model and SATMO-Based Framework

In this study, the orbital thermal behavior of a CubeSat operating in LEO was analyzed using SATMO (Satellite Thermal Model), an open-source orbital thermal analysis tool implemented in MATLAB. SATMO adopts a lumped-parameter thermal modeling approach in which the spacecraft is simplified as a six-sided box, and each surface is represented as a single lumped thermal node.

The six surfaces are defined as Zenith, Nadir, Forward, Aft, North, and South, and the satellite is assumed to maintain a nadir-pointing attitude while traveling along a circular orbit.[5]

For each surface, an energy balance equation was formulated by accounting for time-dependent direct solar flux, Earth albedo, IR radiation, and internal heat generation. The temporal variation of surface temperature was then computed based on this formulation. Radiative heat rejection was modeled according to the Stefan–Boltzmann law, and the surface optical properties α and ε were used as primary input parameters.

The orbital thermal environment varies as a function of the β angle, and eclipse periods were approximated using a cylindrical Earth shadow model. Through this lumped-parameter framework, the temperature response over an orbital period and its sensitivity to variations in optical properties were efficiently evaluated.

2.2 Simulation Setup

The orbital thermal simulations were performed under representative LEO conditions using identical orbital parameters for both BOL and EOL cases. A circular orbit configuration was assumed, and environmental heat inputs including direct solar radiation, Earth infrared emission, and albedo reflection were consistently applied.

Radiation-induced degradation was modeled by modifying the α of the rigid OSR surface based on literature-reported values, while other parameters were maintained constant to isolate the effect of α variation. Transient simulations were conducted over multiple orbital cycles, and temperature responses were evaluated after the third orbit to ensure steady periodic behavior.

Face-wise absorbed heat fluxes, peak temperatures, and temperature amplitudes were extracted to quantify differences between BOL and EOL conditions.

2.3 Analysis Conditions and Input Parameter Definition

Thermal analyses were performed for a six-sided CubeSat operating in LEO. Identical thermophysical and heat capacity properties were assumed for all surfaces, and the primary input parameters used in the simulations are summarized in Tables 1 and 2.

For each surface, the mass was set to 0.085 kg, the area to 0.010 m², and the specific heat to 896 J/kg · K. The initial temperature was assumed to be 20 °C, and a constant internal heat load of 0.33 W was applied.[6] No active heater was used in this study (heater power = 0 W), and bang-bang control was disabled. The solar panels were assumed to be body-fixed with 100% surface coverage. Power generation efficiency was not considered, thereby applying a conservative assumption in which all absorbed solar energy is converted into heat.

Table I: Thermophysical Properties and Satellite Model Parameters Used in the SATMO Analysis.

SATMO field	Input
Satellite face	
Mass, kg	0.085
Area, m²	0.010
Specific heat, J/(kg·K)	896.0
Initial temperature, °C	20.0
Internal heat load, W	0.33
Heater and heater control	
Heater power, W	0.0
Bang-bang control	Off
On trigger, °C	0.0
Off trigger, °C	10.0
Solar panel	
Mounting	Body-Fixed
Face coverage, %	100
Efficiency	0

Table II: Orbital and Environmental Conditions Applied in the Thermal Simulations.[1]

Parameter	Value
Orbit altitude, km	408
Inclination, (°)	51.6
Beta angle (Hot case), (°)	60
Beta angle (Cold case), (°)	0
Solar flux, W/m²	1367
Albedo factor	0.3
Sun-side IR planetsine, W/m²	236
Dark-side IR planetsine, W/m²	236
Simulation duration, s	518400
Time step, s	1
Primary body	Earth

The orbital altitude was set to 408 km with an inclination of 51.6°. The β angle was adopted as the primary environmental parameter, with the hot case defined as β = 60° and the cold case as β = 0°. The solar constant was assumed to be 1367 W/m², and the albedo factor was set to 0.3. IR radiation was uniformly prescribed as 236 W/m² for both sunlit and eclipse conditions.

The simulation was conducted for a total duration of 518,400 s (approximately six orbital periods) with a time step of 1 s. The temperature response was analyzed after the system reached a steady periodic state.

2.4 Optical Property Degradation Conditions and Comparison Scenarios

To evaluate the impact of radiation-induced optical property changes, three representative passive thermal

control materials were analyzed under BOL and EOL conditions (Table 3 and 4).

Table III: BOL and EOL Infrared Emittance (ε).[4]

Sample	ε (BOL)	ε (EOL)
Rigid OSR 1	0.861	0.862
Flexible OSR with ITO	0.861	0.883
White paint - 3	0.955	0.942

Table IV: BOL and EOL Solar Absorptance (α).[4]

Sample	α (BOL)	α (EOL)
Rigid OSR 1	0.040	0.043
Flexible OSR with ITO	0.061	0.134
White paint - 3	0.251	0.639

The materials considered in this study were Rigid OSR, Flexible OSR with ITO, and White paint. The corresponding ε and α values under BOL and EOL conditions are summarized in Tables 3 and 4, respectively.

For the Rigid OSR, the infrared emittance exhibited negligible variation (0.861 → 0.862), while α slightly increased (0.040 → 0.043). In the case of Flexible OSR, the emittance increased from 0.861 to 0.883, accompanied by a more pronounced increase in α from 0.061 to 0.134. For White paint, the emittance decreased from 0.955 to 0.942, whereas α significantly increased from 0.251 to 0.639.

Thermal analyses were performed for each material under both BOL (initial α and ε) and EOL (degraded α and ε) conditions for the hot case (β = 60°) and cold case (β = 0°). This framework enabled quantitative assessment of the impact of optical property degradation on orbital temperature distributions and peak temperatures (T_max).

3. Results and Discussion

Figures 2–4 present the surface temperature histories of the six CubeSat faces under hot (β = 60°) and cold (β = 0°) conditions for each material (Rigid OSR, Flexible OSR with ITO, and White paint, respectively). All comparisons were performed after the system reached a steady periodic state.

3.1 Hot Case (β = 60°) Analysis

Under the hot-case condition, the peak temperature (T_max) among the six surfaces was selected as the primary comparison parameter between BOL and EOL conditions. The magnitude of temperature increase differed significantly depending on the material.

As shown in Figure 2, for Rigid OSR (OSR1), T_max increased from −51.745°C to −51.332°C, corresponding to a temperature rise of 0.41 K. Based on the allowable operating range of [−75 to 100°C], the hot thermal margin decreased by only 0.27%, indicating a negligible influence of radiation-induced degradation of optical properties.[7]

As shown in Figure 3, for Flexible OSR (FOSR), T_max increased from −48.741°C to −39.734°C, representing a temperature rise of 9.01 K. Consequently, the hot thermal margin decreased by 6.06%, confirming that changes in optical properties exert a substantial impact on temperature elevation.

As shown in Figure 4, for White paint (WP3), T_max increased from −28.205°C to 10.040°C, resulting in a significant rise of 38.24 K. This represents the largest variation among the three materials, with the hot thermal margin reduced by 29.83%. Notably, under EOL conditions, the temperature exceeded 0 °C, indicating that radiation-induced degradation of optical properties may drive the system closer to its upper operational limit.

The absorbed heat flux distributions (Figure 4) indicate that, under EOL conditions, the increase in α substantially amplified contribution from direct solar radiation and albedo. This enhanced heat absorption was identified as the primary driver of the increase in T_max.

3.2 Cold Case (β = 0°) Analysis

Under cold-case conditions, the minimum temperature (T_min) among the six surfaces was used for comparison.

As illustrated in Figure 2, for OSR1, T_min increased slightly from −56.951°C to −56.707°C, corresponding to a rise of 0.24 K. The cold thermal margin changed by −1.35%, indicating minimal practical impact.

As illustrated in Figure 3, for FOSR, T_min increased from −55.095°C to −49.824°C, resulting in a temperature rise of 5.27 K. The cold thermal margin changed by −26.48%, indicating that degradation shifts the temperature distribution upward even under cold conditions.

As illustrated in Figure 4, for WP3, T_min increased from −44.252°C to −24.408°C, corresponding to a rise of 19.84 K. The cold thermal margin changed by −64.54%, representing the largest reduction in thermal margin among the evaluated materials.

Similar to the hot-case results, materials exhibiting larger optical property variations demonstrated more pronounced temperature shifts under cold conditions.

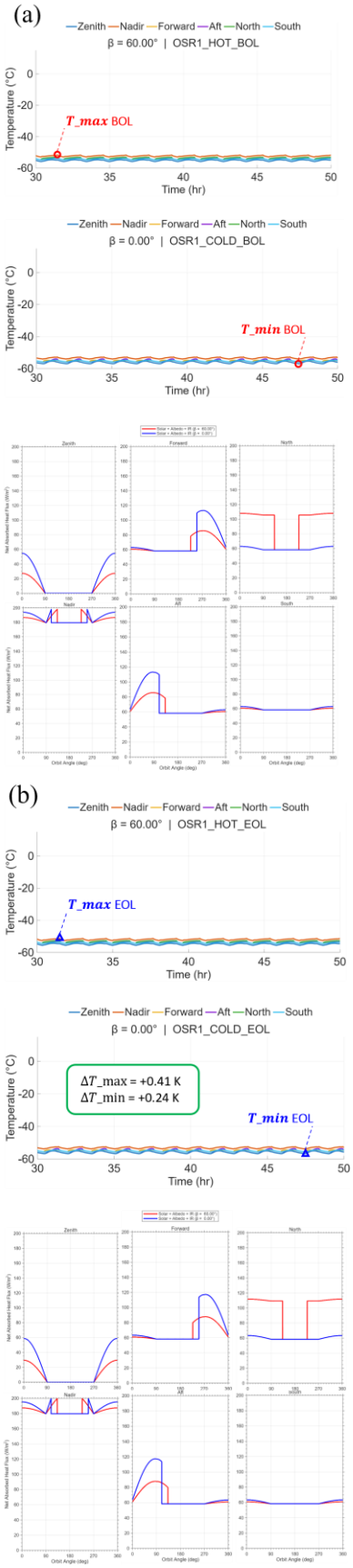

Fig. 2. Comparison of surface temperature responses and absorbed heat flux distributions under BOL (a) and EOL (b) conditions for Rigid OSR under hot and cold β-angle conditions.

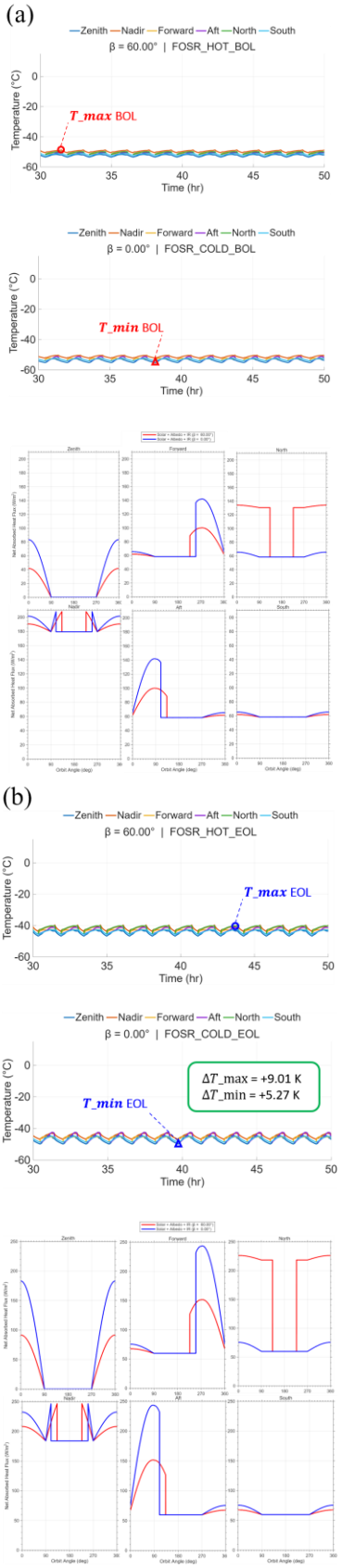

Fig. 3. Comparison of surface temperature responses and absorbed heat flux distributions under BOL (a) and EOL (b) conditions for Flexible OSR with ITO under hot and cold β-angle conditions.

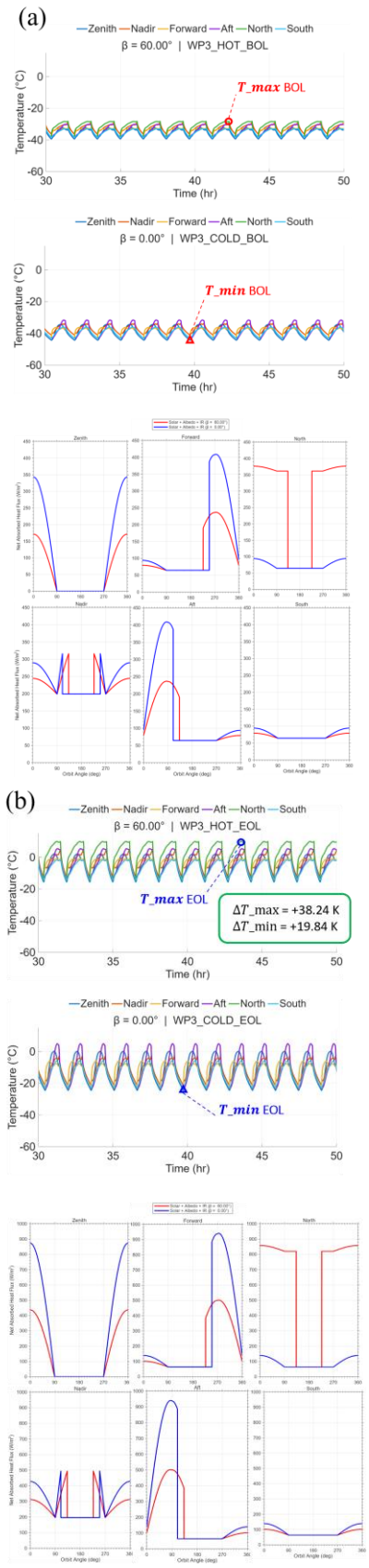

Fig. 4. Comparison of surface temperature responses and absorbed heat flux distributions under BOL (a) and EOL (b) conditions for White paint under hot and cold β-angle conditions.

3.3 Overall Comparison

The comparison of BOL and EOL conditions revealed that the increase in T_max under the hot case followed the trend:
OSR1 (0.41 K) < FOSR (9.01 K) < WP3 (38.24 K).

A similar tendency was observed for T_min (OSR1: 0.24 K; FOSR: 5.27 K; WP3: 19.84 K), indicating that optical property degradation does not merely affect the extreme temperature values but shifts the entire orbital temperature range upward.

In particular, as evident in Figure 4, the substantial increase in α (from 0.251 to 0.639) for White paint, combined with a decrease in ε, resulted in simultaneous enhancement of heat absorption and reduction of radiative heat rejection. This dual effect amplified the temperature rise. In contrast, Rigid OSR (Figure 2) exhibited minimal changes in α and ε, leading to negligible variation in thermal behavior.

These results demonstrate that radiation-induced radiation-induced degradation of optical properties induces material-dependent thermal responses and, in certain cases, may lead to a significant reduction in thermal safety margin.

4. Conclusions

In this study, the impact of radiation-induced optical property degradation on the orbital temperature behavior of a CubeSat was quantitatively evaluated using a SATMO-based lumped-parameter orbital thermal analysis framework. Three representative passive thermal control materials—Rigid OSR, Flexible OSR, and White paint—were analyzed under BOL and EOL conditions, and their thermal responses were compared under β = 60° and β = 0°.

The results indicate that for Rigid OSR, which exhibited minimal optical property variation, the changes in T_max and T_min were limited to 0.41 K and 0.24 K, respectively, suggesting negligible thermal impact. In contrast, Flexible OSR showed temperature increases of 9.01 K in T_max and 5.27 K in T_min, while White paint exhibited the largest temperature rise, with T_max increasing by 38.24 K and T_min by 19.84 K. In particular, for White paint, the hot thermal margin decreased by 29.83%, and the cold thermal margin changed by −64.54%, confirming that radiation-induced changes in optical properties can significantly affect thermal safety margins.

A comparative assessment of the three materials revealed that larger variations in optical properties resulted in proportionally greater increases in T_max and T_min. This indicates that radiation-induced degradation does not merely alter extreme temperature values but shifts the entire orbital temperature range upward. In cases where an increase in α coincided with a decrease in ε, the combined effects of enhanced heat absorption and reduced radiative heat rejection amplified the overall temperature rise.

These findings suggest that thermal designs based solely on initial (BOL) optical properties may overestimate long-term thermal safety under extended mission conditions. Therefore, EOL-based thermal analyses that account for radiation-induced degradation of optical properties should be incorporated into the design process for long-duration and thermal margin assessment.

In addition, this study can be regarded as a preliminary investigation for space nuclear power systems, where accurate prediction of external thermal environments is essential for defining boundary conditions for onboard systems.

The proposed framework can be further extended to system-level thermal analyses and long-term orbital reliability assessments of space nuclear applications through integration with higher-fidelity three-dimensional thermal models.

Acknowledgement

This work was supported by the National Research Foundation of Korea (NRF) grant funded by Korea government (MSIT) (RS-2025-02310831)

REFERENCES

[1] Kim, K. M., Lee, M. K., & Park, S. H. (2025). Thermal Control Design and Analysis Techniques for Reliable Mission Operations of CubeSat. Journal of Space Technology and Applications, 5(3), 125-138.

[2] Katelyn, E. B. (2018). Thermal Analysis and Control of Small Satellites in Low Earth Orbit. Missouri University of Science and Technology, MO.

[3] National Aeronautics and Space Administration (NASA). State-of-the-Art of Small Spacecraft Technology: 7.0 Thermal Control. NASA Small Spacecraft Systems Virtual Institute. Available from https://www.nasa.gov/smallsat-institute/sst-soa/thermal-control/

[4] Sharma, A. K., & Sridhara, N. (2012). Degradation of thermal control materials under a simulated radiative space environment. Advances in space research, 50(10), 1411-1424.

[5] Chipps, A., Forgette, D., & Cahoy, K. (2026). SATMO: a Multi-Planet Thermal Analysis Tool for CubeSat Missions. In AIAA SCITECH 2026 Forum (p. 2269).

[6] Saddul, K., Saletes, J., Kim, M., & Wittig, A. (2024). Mission analysis of a 1U CubeSat post-mission disposal using a thin-film vacuum arc thruster. Acta Astronautica, 219, 318-328.

[7] Mason, J. P., Lamprecht, B., Woods, T. N., & Downs, C. (2018). CubeSat on-orbit temperature comparison to thermal-balance-tuned-model predictions. Journal of thermophysics and heat transfer, 32(1), 237-255.